

Original article

Numerical study of vug effects on acid-rock reactive flow in carbonate reservoirs

Zhaoqin Huang¹*, Hongchuan Xing¹, Xu Zhou², Haoyu You²

¹School of Petroleum Engineering, China University of Petroleum (East China), Qingdao 266580, P. R. China

²Research Institute of Exploration and Development, Xinjiang Oilfield Company, PetroChina, Karamay, Xinjiang 834000, P. R. China

Keywords:

Acid-rock reaction
Navier-Stokes/Darcy Equations
two-scale model
acidizing process

Cited as:

Huang, Z., Xing, H., Zhou, X., You, H. Numerical study of vug effects on acid-rock reactive flow in carbonate reservoirs. *Advances in Geo-Energy Research*, 2020, 4(4): 448-459, doi: 10.46690/ager.2020.04.09.

Abstract:

Matrix acidizing is one of the most practical stimulation technologies for carbonate reservoirs, which effectively improve the region permeability near the wellbore. In addition to solid matrix, vugs are also very common in carbonate reservoirs. However, a few studies have been addressed with existence of vugs on carbonate acidizing process. In this work, a two-scale model is developed using dual domain method and discrete vugs model to study effect of vugs on acidizing process. Darcy equation is employed in solid matrix region. Navier Stokes equation is adopted for free flow region in vugs. The two regions are coupled by modified Beavers-Joseph-Saffman boundary condition. Numerical cases are conducted to present the effect of vug characteristics on acid-rock reaction process. The results show that acid solution has the largest effective reducing distance and the smallest breakthrough volume in circular vugs. Dominant wormhole is created when acid injection direction is parallel or vertical to the azimuth angle of vugs. Increasing amount of vugs in horizontal effectively reduces the flow distance and breakthrough volume of acid solution. Vugs with random distribution increases effective flow distance and breakthrough volume of acid solution compared to vugs with orderly distribution.

1. Introduction

Carbonate reservoir is one of the most important reserves in the world. China has rich marine carbonate oil and gas resources with 4.5×10^6 m² distribution area and 3.58×10^8 t oil equivalent (Zhang et al., 2017; Kang et al., 2020). According to storage types, marine carbonate reservoirs can further be divided into three types: porous media reservoir, fractured-porous media reservoir and fractured-vuggy media reservoir (Yang, 2013). Fractured-vuggy media reservoir accounts for 30% of the total (Ma et al., 2017). Different from porous media and fractured-porous media carbonate reservoirs, fractured-vuggy reservoir has great different reservoir space and flow pattern. Three types of reservoir space including matrix pores, fractures, and vugs, coexist with strong heterogeneity and spatial distribution scale is varying from millimeter to meter. Moreover, flow laws in fractured-vuggy reservoir are also very complex including seepage process in porous media region and free seepage in dissolution vugs (Huang et al., 2010, 2011; Huang, 2012; Li, 2017; Wang et al., 2017; Cai and Hu, 2019).

Matrix acidizing is one of the main reconstruction technologies for fractured-vuggy carbonate reservoirs, which can effectively improve the permeability near the wellbore. Over the past several decades, lots of studies have been conducted to study carbonate acidizing process from physical experiment and numerical simulation. Dolomite and calcite rotating disk experiment results show that that both mass transfer and surface reaction rate limit the dissolution rate (Lund et al., 1973, 1975). Daccord et al. (1993) developed an equivalent size parameter based on Darcy's law to describe the flow characteristics of wormhole pattern. Wang et al. (1993) found that the optimal acid rate was a function of rock composition, reaction temperature and pore size distribution of virgin formation rocks through laboratory core-flooding experiments. Fredd and Fogler (1998, 1999) presented a lot of core acidizing experiments according to different acid injection rates and obtained different wormhole patterns. Based on their experimental results, Fredd and Miller (2000) divided the wormhole dissolution patterns into five categories: face dissolution, conical wormhole, dominant wormhole, ramified

wormhole and uniform dissolution. Panga et al. (2002, 2005) developed a new averaged model to describe the flow and reaction in porous media. And then they established a two-scale continuous model to describe transport and reaction mechanisms. In addition, different dissolution patterns observed in core acidification experiments are reproduced by using the model in two-dimensional domain. Furthermore, McDuff et al. (2010) realized the acidizing experiments on large-scale carbonate cores and captured three-dimensional (3D) wormhole patterns by high-resolution CT imaging.

Izgec et al. (2010) used Darcy-Brinkman equation to study the flow law of acid in vuggy reservoirs. They investigated the effect of single vug and different distribution of multiple vugs. Based on Darcy's law, Liu et al. (2016) introduced the variation function model to study the influence of core pore structure on the 3D multi-scale wormhole expansion in carbonate rocks. They analyzed the effects of pore-scale heterogeneities and spatial distribution of pore structure on pore volume breakthrough and wormhole propagation. Qi et al. (2019) studied the influence of fracture strike and different fracture shapes on acid wormhole propagation in fractured-vuggy reservoirs by combining two-scale model and pseudo fracture model. But, their study did not consider the effect of dissolution vugs. Yuan et al. (2019) established a 3D numerical model using Stokes-Brinkman equation to study fluid flow law and chemical reaction in fractured carbonate formation. And on this basis, they studied the effects of heterogeneity of porous media and mineral volume fractions on the alterations of rock properties and dissolution patterns. Ali et al. (2020) studied the influence of natural fractures, vugs and the coexistence of vugs and fractures on matrix acidification by using Navier-Stokes equation under two-dimensional radial condition. Zhao et al. (2020) studied the influence of spatial distribution of natural micro fractures on wormhole propagation based on the two-scale model coupled with Monte Carlo method. However, the numerical simulation results have not been verified by physical experiments. For the simulation of acid flow in the matrix, most researchers use single domain method, in which only one system equation Brinkman/Navier Stokes system or Navier Stokes/Forchheimer system is used in the whole system. However, this method is limited to the description of the transition interface between the matrix system and the vug system. Moreover, Laplacian term may also not be suitable for the low velocity case (Nield and Bejan, 2013).

In this work, discrete fracture-vug model (Yao et al., 2010; Zheng et al., 2010) is used to describe acid flow, in which Darcy equation is employed in solid matrix region and Navier Stokes equation is adopted for free flow region in vugs. The modified Beavers-Joseph-Saffman (BJS) boundary conditions are introduced to couple the matrix rock system and dissolution vug system. Lots of numerical cases are conducted to study the effect of the existence of dissolution vugs on the propagation of acid wormhole in carbonate formation.

2. Two-scale mathematical model for matrix media

2.1 Darcy scale model

The flow of fluid in porous media can be expressed by Darcy's law:

$$\mathbf{v} = -\frac{K}{\mu} \nabla P \quad (1)$$

where \mathbf{v} is a vector to express the Darcy velocity, m/s; K is a tensor to express the permeability of the study area, m^2 ; μ is the viscosity of the fluid, $\text{mPa}\cdot\text{s}$; P is the pressure of the fluid, Pa. The continuity equation is derived from the law of conservation of mass and the formula is as follow:

$$\frac{\partial \phi}{\partial t} + \nabla \cdot \mathbf{v} = 0 \quad (2)$$

where ϕ is the porosity of carbonate rocks, t is the acid-rock reaction time.

The transport equation of solute in liquid phase is expressed by the following mass balance equation:

$$\frac{\partial(\phi C_f)}{\partial t} + \nabla \cdot (\mathbf{v} C_f) = \nabla \cdot (\phi D_e \cdot \nabla C_f) + R \quad (3)$$

where C_f is the concentration of acid in the liquid phase, mol/m^3 ; D_e is the diffusion coefficient tensor, m^2/s ; R is the reaction term, which is determined by:

$$R = -a_v \cdot k_c (C_f - C_s) \quad (4)$$

where a_v is the specific surface area of carbonate rocks, m^{-1} ; k_c is the mass transfer coefficient of acid solution, m/s ; C_s is the concentration of acid solution on the surface of liquid and solid in core pores, mol/m^3 . C_s is expressed as:

$$C_s = \frac{C_f}{1 + \frac{k_s}{k_c}} \quad (5)$$

Chemical reactions between rocks and acids lead to the change of porosity of carbonate rocks. The dynamic change with reaction of porosity is determined by:

$$\frac{\partial \phi}{\partial t} = \frac{a_v \cdot \alpha \cdot k_c (C_f - C_s)}{\rho_s} \quad (6)$$

where α is corrosion ability of acid solution, kg/mol ; ρ_s is the density of carbonate rocks, kg/m^3 .

2.2 Pore scale model

Porosity, pore radius and specific surface area of rocks are related to pore structure. Reaction between acid solution and rock continuously dissolves porous media and changes the pore structure of rocks resulting in dynamic changes of various physical parameters of carbonate rocks. The calculation methods of various physical parameters of rocks in acid rock reaction can be divided into two types. One is to observe the dynamic changes of pore structure of real core in the process of acid rock reaction, and then calculate other physical

parameters of rock. Another method is to calculate various physical parameters of rock according to empirical or semi-empirical formula. The latter is usually adopted in numerical studies on acidizing process (Panga et al., 2005; Kalia and Balakotaiah, 2009; Maheshwari et al., 2013; Ghommem et al., 2015). Based on the modified Carman-Kozeny equation (Panga et al., 2005), the change of porosity and permeability can be expressed as:

$$\begin{cases} \frac{k}{k_0} = \frac{\phi}{\phi_0} \left[\frac{\phi(1-\phi_0)}{\phi_0(1-\phi)} \right]^{2\beta} \\ \frac{r_p}{\bar{r}_0} = \sqrt{\frac{k\phi_0}{k_0\phi}} \\ \frac{a_v}{\bar{a}_0} = \frac{\phi\bar{r}_0}{\phi_0 r_p} \end{cases} \quad (7)$$

where r_p is the average pore radius of porous media, m; \bar{r}_0 is the initial value of average pore radius; \bar{a}_0 is the initial value of interfacial area of carbonate rocks, m^{-1} ; k_0 is the initial permeability of cores, m^2 ; ϕ_0 is the initial porosity of cores; the parameter β is a constant to extend the relation to a dissolving medium.

Velocity of solute transport from liquid phase to pore surface and contact with pore wall can be expressed by mass transfer velocity. Eq. (5) shows that the mass transfer rate has a great influence on the acid rock reaction. Its magnitude affects the chemical reaction and directly determines whether the chemical reaction is in the stage of dynamic control reaction or mass transfer control reaction. Many literature studies have illustrated that the mass transfer coefficient of acid solution in acid rock reaction is related to the properties of rock itself, reaction rate of injected acid and convection velocity of acid solution in porous media. Sherwood number (Panga et al., 2005) is a dimensionless number, also known as dimensionless mass transfer coefficient, which correlates these factors. Sherwood number can be expressed as:

$$Sh = \frac{2k_c \bar{r}_p}{D_m} = Sh_\infty + b Re_p^{1/2} Sc^{1/3} \quad (8)$$

where \bar{r}_p is the average pore radius of porous media, m; D_m is the molecular diffusion coefficient, m/s^2 ; Sh_∞ is the asymptotic Sherwood number of pores, b is a constant related to the surface of porous media, and $B = 0.7/m^{1/2}$, where m is the ratio of the length to the radius of the pore; Re_p is the pore Reynolds number, which can be expressed as $Re_p = 2ur_p/\nu$: where ν is the hydrodynamic viscosity; Sc is the Schmidt number defined as $Sc = \nu_k/D_m$, where ν_k is hydrodynamic viscosity.

The two terms on the far right of Eq. (8) represent the contribution of convection and diffusion of acid solution to Sherwood number. According to its expression, the diffusion term is related to the geometry of the pore and the convection term is an equation related to the local velocity field. The studies (Balakotaiah and West, 2002) on the asymptotic Sherwood number illustrate that Sh_∞ is related to the shape of the cross-section of the pore. Sh_∞ values 2.98 when the cross section of pore is square. Sh_∞ values 2.50 when the cross section of

pore is triangle. Sh_∞ values 3.66 when the cross section of pore is circular. In this work, $Sh_\infty = 3$, is adopted for numerical simulation. The convection term is related to the Reynolds number and Schmidt number of pores. For fluid, the studies show that Schmidt's value is about 1,000.

It can be seen from Eq. (8) that the Reynolds number of pores is directly proportional to the pore radius of porous media and the injection rate of acid solution. When both are extremely small, the value of pore Reynolds number is also very small. In this case, the effect of convection term can be ignored in dimensionless diffusion coefficient. The effect of convection term on mass transfer rate is changing with different processes of dissolution reaction. When convection plays a dominant role, porosity is comparatively large. But, the specific surface area of rocks is very small, which results in the effect of convective mass transfer on chemical reaction can be negligible. When the velocity of acid entering the core is very high in the entrance section, the convective mass transfer plays a decisive role in the acid rock reaction.

2.3 Diffusion coefficient of acid solution

When acid solution is transported in a homogeneous anisotropic matrix, diffusion coefficient can be expressed by axial diffusion coefficient D_{eX} and lateral diffusion coefficient D_{eT} in two-dimensional space. In the case of no flow, only molecular diffusion exists in solute, and the transverse diffusion coefficient is equal to the axial diffusion coefficient which can be expressed as:

$$D_{eX} = D_{eT} = \alpha_{os} D_m \quad (9)$$

where D_m is the molecular diffusion coefficient, m/s^2 ; α_{os} is a constant related to the structure of porous media. The two-dimensional diffusion coefficient of acid is related to the geometry of porous media the flow pattern of pore scale and the properties of acid solution when acid solution flows in porous media. The ratio of convection to diffusion is defined by the dimensionless Peclet number. Peclet number can be expressed as:

$$Pe_p = \frac{|v|d_h}{\phi D_m} \quad (10)$$

where $|v|$ is the value of Darcy velocity, m/s; d_h is the pore diameter of porous media, m.

The diffusion coefficient formula derived by Panga is used to describe the diffusion of acid in porous media. Axial diffusion coefficient and transverse diffusion coefficient (Panga et al., 2005) can be expressed as:

$$D_{eX} = \alpha_{os} D_m + \lambda_X D_m Pe_p \quad (11)$$

$$D_{eT} = \alpha_{os} D_m + \lambda_T D_m Pe_p \quad (12)$$

where the subscripts X and T denote the direction of acid injection and the transverse direction, respectively, λ_X and λ_T are constants related to pore structure of porous media (for spherical fillers, $\lambda_X = 0.5$, $\lambda_T = 0.1$).

2.4 Initial and boundary conditions

When a certain pressure is applied at the outlet, it is a constant pressure boundary. And the upper and lower boundaries are closed boundaries. The specific boundary condition can be expressed as:

$$P = 0, C_f = 0, \quad \text{at } t = 0 \quad (13)$$

$$u_0 = -\frac{k_x}{v} \frac{\partial P}{\partial x}, \frac{\partial P}{\partial y} = 0, C_f = C_0, \quad \text{at } x = 0 \quad (14)$$

$$\frac{\partial C_f}{\partial x} = 0, P = P_e, \quad \text{at } x = L \quad (15)$$

$$\frac{\partial P}{\partial y} = 0, \frac{\partial C_f}{\partial y} = 0, \quad \text{at } y = 0 \text{ and } y = L \quad (16)$$

where u_0 is initial injection rate, m/s; C_0 is the acid injection concentration at the inlet, mol/m³; P_e is a constant representing the outlet boundary pressure, Pa.

2.5 Dimensionless mathematical model

There are many factors influencing acid rock reaction. To make the numerical solution of acid rock reaction easier, the mathematical model is dimensionless to eliminate the influence of dimension. The dimensionless expression of each parameter is shown below:

$$x^* = \frac{x}{L}, y^* = \frac{y}{L}, U^* = \frac{v}{u_0}, t^* = \frac{t}{L/u_0}, r_p^* = \frac{r_p}{\bar{r}_0}, a_v^* = \frac{a_v}{\bar{a}_0},$$

$$K^* = \frac{K}{k_0}, D^* = \frac{D_e}{D_m}, C_f^* = \frac{C_f}{C_0}, P^* = \frac{P - P_e}{(\mu u_0 L) / K_0}, h_T^2 = \frac{2k_s \bar{r}_0}{D_m},$$

$$Da = \frac{k_s \bar{a}_0 L}{u_0}, Pe_L = \frac{u_0 L}{D_m}, N_{ac} = \frac{\alpha C_0}{\rho_s}, \Phi^2 = \frac{k_s \bar{a}_0 L^2}{D_m}, \eta = \frac{2r_0}{L}.$$

where the superscript * indicates dimensionless, L is characteristic length of research area in mathematical model, x and y are rectangular coordinate system parameters, U^* is dimensionless velocity vector, K^* is dimensionless permeability parameters.

After dimensionless mathematical equation, a new set of dimensionless variables is obtained. Thiele modulus h_T^2 is the ratio of acid reaction velocity and diffusion velocity in pore volume of porous media in initial state. N_{ac} is a constant indicating the acidizing ability of acid solution. Pe_L is axial Peclet number indicating the ratio of acid injection velocity to diffusion velocity. Damköhler number Da (Fredd et al., 1997) is the ratio of reaction velocity to convection velocity at core scale. Macroscopic Thiele modulus Φ^2 is related to Da and Pe_L , which can be expressed as:

$$\Phi^2 = \frac{k_s \bar{a}_0 L^2}{D_m} \quad (17)$$

Macroscopic Thiele modulus is the equivalent expression of pore scale Thiele modulus at core scale. The Eq. (17) shows that the macroscopic Thiele modulus has little to do with the acid injection rate. By substituting the above dimensionless

parameters into the Eq. (1)-(3), the dimensionless equation can be expressed as:

$$U^* = -K^* \cdot \nabla P_D \quad (18)$$

$$\frac{\partial \phi}{\partial t^*} + \nabla \cdot U^* = 0 \quad (19)$$

$$\frac{\partial (\phi C_f^*)}{\partial t^*} + \nabla \cdot (U^* C_f^*) = \nabla \cdot (D^* \cdot \nabla C_f^*) - \frac{Da \cdot a_v^* \cdot C_f^*}{1 + \frac{h_T^2 \cdot r_p^*}{Sh}} \quad (20)$$

The change of dimensionless porosity can be expressed as:

$$\frac{\partial \phi}{\partial t^*} = \frac{Da \cdot N_{ac} \cdot a_v^* \cdot C_f^*}{1 + \frac{h_T^2 \cdot r_p^*}{Sh}} \quad (21)$$

Dimensionless formula of diffusion coefficient D^* can be expressed as:

$$D^* = (D_x, D_y) = \left(\frac{\alpha_{os} \phi Da}{\Phi^2} + \lambda_x |U| r_p^* \eta \right)^T \quad (22)$$

The above equations are a dimensionless mathematical model to describe the reactive flow of acid solution in rocks. The dimensionless boundary conditions and initial conditions can be expressed as:

$$\left\{ \begin{array}{l} U^*|_{\text{injection boundary}} = 1 \\ P^*|_{\text{outer boundary}} = 1 \\ \frac{\partial P^*}{\partial \bar{n}}|_{\text{outer boundary}} = 0 \\ C_f^*|_{\text{injection boundary}} = 1 \\ \frac{\partial C_f^*}{\partial \bar{n}}|_{\text{outer boundary}} = 0 \\ \frac{\partial P^*}{\partial \bar{n}}|_{\text{horizontal boundary}} = 0 \\ \left\{ \begin{array}{l} C^*|_{t^*=0} = 0 \\ U^*|_{t^*=0} = 0 \end{array} \right. \end{array} \right. \quad (23)$$

3. Mathematical model of acid rock reaction in vuggy media

3.1 Mathematical model of vug system

Vug system belongs to free flow region and flow of fluid in vug system can be expressed by N-S equation. The continuity equation in vugs can be expressed as:

$$\frac{\partial \rho}{\partial t} + \nabla \cdot (\rho v_s) = 0 \quad (25)$$

where v_s is the velocity vector of acid in vug area, m/s. The subscript s denotes free flow. N-S equation can be expressed as:

$$\rho \left[\frac{\partial v_s}{\partial t} + (v_s \cdot \nabla) v_s \right] = \nabla \cdot \sigma_s + \rho g \quad (26)$$

where σ_s is the stress of free flow fluid, Pa; g is acceleration of gravity, m/s². And σ_s can be expressed as:

$$\sigma_s = -P_s I + \mu \left[\nabla v_s + (\nabla v_s)^T \right] \quad (27)$$

where P_s is the pressure of acid solution in vugs, Pa; I is the unit matrix. Because the velocity is very small, the influence of inertia term is ignored in this equation. The second term on the right of Eq. (27) is defined as:

$$\tau = \mu \left[\nabla v_s + (\nabla v_s)^T \right] \quad (28)$$

The convection diffusion equation of acid solution in vugs can be expressed as:

$$\frac{\partial C_s}{\partial t} + \nabla \cdot (v_s C_s) - \nabla \cdot (D_{e,s} \cdot \nabla C_s) = 0 \quad (29)$$

where C_s is concentration of acid solution in vugs, mol/m³; $D_{e,s}$ is the effective diffusion coefficient tensor of acid solution in vugs, m²/s. The axial and transverse effective diffusion coefficients of acid solution in vugs can be expressed as:

$$D_{eX,s} = \alpha_{eX} \cdot v_{x,s} + D_m \quad (30)$$

$$D_{eT,s} = \alpha_{eT} \cdot v_{T,s} + D_m \quad (31)$$

3.2 Interface coupling condition

Matrix system and vug system are two different scales, which involve Stokes-Darcy coupling problem. Due to the different order of differential equations, it is necessary to introduce appropriate interface conditions on the interface. In this work, the modified BJS condition is introduced to couple matrix rock block system and vug system. The expression of modified BJS condition is as follow:

$$\begin{cases} v_s \cdot n = v_d \cdot n \\ P_s - n \cdot \tau \cdot n = P_d \\ -n \cdot \tau \cdot t = \frac{\mu \beta}{\sqrt{t \cdot K \cdot t}} (v_s - v_d) \cdot t \end{cases} \quad (32)$$

where n is the unit vector of interface; t is the unit tangent vector; P_d is pressure in matrix, Pa; P_s is pressure in vugs, Pa; τ is the shear stress tensor; β is velocity slip coefficient. The subscripts s and d represent Stokes and Darcy flows respectively. The first condition is the normal velocity continuity condition. The second condition is the normal stress continuous condition. The third is the famous beavers Joseph (BJ) velocity slip condition (Beavers and Joseph, 1967; Saffman, 1971; Taylor, 1971; Mosthaf et al., 2011). The convection

diffusion equations between the two regions are continuously coupled by concentration:

$$C_f|_{\text{matrix boundary}} = C_s|_{\text{vug boundary}} \quad (33)$$

3.3 Dimensionless parameter

The dimensionless parameters of vug system are derived as follows:

$$\begin{aligned} x^* &= \frac{x}{L}, y^* = \frac{y}{L}, U^* = \frac{v}{u_0}, t^* = \frac{t}{(L/u_0)}, r_p^* = \frac{r_p}{\bar{r}_0}, a_v^* = \frac{a_v}{\bar{a}_0}, \\ K^* &= \frac{K}{k_0}, D^* = \frac{D_e}{D_m}, C_f^* = \frac{C_f}{C_0}, P^* = \frac{P - P_e}{(\mu u_0 L)/K_0}, h_T^2 = \frac{2k_s \bar{r}_0}{D_m}, \\ Da &= \frac{k_s \bar{a}_0 L}{u_0}, Pe_L = \frac{u_0 L}{D_m}, N_{ac} = \frac{\alpha C_0}{\rho_s}, \Phi^2 = \frac{k_s \bar{a}_0 L^2}{D_m}, \eta = \frac{2\bar{r}_0}{L}, \\ U_f^* &= \frac{v_f}{u_0}, B = \frac{d}{L}, K^* = \frac{K_f}{k_0}, D_f^* = \frac{D_{e,f}}{D_m}, U_s^* = \frac{v_s}{u_0}, \\ F^* &= \frac{\rho g}{\rho \cdot u_0^2 / L}, P_s^* = \frac{P_s}{\rho u_0^2}, D_s^* = \frac{D_{e,s}}{D_m}, Re = \frac{\rho u_0 L}{\mu}. \end{aligned}$$

where F^* is dimensionless body force; D_s^* is dimensionless diffusion coefficient of dissolution vugs; Re is Reynolds number.

Using the above parameters, the dimensionless mathematical model of vug system can be expressed as:

$$\nabla \cdot (U_s^*) = 0 \quad (34)$$

$$\frac{\partial U_s^*}{\partial t^*} = \nabla \cdot (P_s^* I + \tau^*) + F^* \quad (35)$$

$$\tau^* = \frac{1}{Re} \left[\nabla U_s^* + (\nabla U_s^*)^T \right] \quad (36)$$

$$\frac{\partial C_s^*}{\partial t^*} + \nabla \cdot (U_s^* C_s^*) - \nabla \cdot (D_s^* \cdot \nabla C_s^*) = 0 \quad (37)$$

$$D_s^* = (D_x^*, D_y^*) = \begin{pmatrix} \alpha_{os} |U_x^*| + \frac{1}{Pe_L} \\ \alpha_{os} |U_y^*| + \frac{1}{Pe_L} \end{pmatrix}^T \quad (38)$$

The dimensionless conditions of concentration coupling between seepage and free flow regions can be expressed as:

$$C_f^*|_{\text{matrix boundary}} = C_s^*|_{\text{vug boundary}} \quad (39)$$

Table 1. The parameters and values in numerical simulation.

Parameters	Practical significance	Value	Unit
ρ_L	Acid density	1.1	g/cm ³
C_0	Acid injection concentration at the inlet	6.02	mol/L
μ	Acid viscosity	1	mPa·s
D_m	Molecular diffusion coefficient	3.6e-6	cm ² /s
k_s	Surface reaction rate constant	0.001	cm/s
k_0	the initial permeability of the core	1×10^{-3}	μm^2
ϕ_0	the initial porosity of the core	0.3	
$\Delta\phi_0$	Porosity variation	0.15	
a_0	Interfacial area	100	cm ² /cm ³
\bar{r}_0	Initial average pore radius	0.0005	cm
ρ_s	Rock density	2.7	g/cm ³
L	Length of the model	10	cm
W	Width of the model	4	cm
λ_X	Longitudinal pore structure efficient	0.5	
λ_T	Transverse pore structure coefficient	0.1	
α_{os}	Pore-structure constant	0.5	
SH_∞	Asymptotic Sherwood number	3	
h_T^2	the ratio of acid reaction velocity and diffusion velocity	0.005	
S_C	Schmidt number	252.53	
N_{ac}	Acid capacity number	0.1	
Φ^2	Macroscopic Thiele modulus	34722	
η	Ratio of the pore scale to the core sample scale	4e-5	

4. Numerical studies on acid rock reaction based on discrete vug model

The numerical methods for solving the reactive flow problem mainly include finite difference method, finite element method and finite volume method (MacQuarrie and Mayer, 2005). In this work, the finite element method is applied to solve the mathematical model of acid-rock reactive flow. Firstly, the porosity, permeability, specific surface area and mass transfer coefficient of the model were calculated according to the initial conditions. The time is recorded as t , and the concentration field is calculated by convection diffusion equation. The porosity field at time $t+1$ is calculated by Eq. (21). The Darcy velocity field is updated according to the change of porosity, and then the concentration field is updated according to the change of Darcy velocity field. Repeat the above calculation steps until the acid solution breaks through the core.

Using the above mathematical model and numerical calculation method, the acid-rock reactive flow in dissolution vug media is simulated based on the discrete vug model under two-dimensional conditions. The values of numerical simulation parameters are shown in Table 1. In each simulation case, the displacement velocity under the condition of wormhole formation is studied until the core achieves breakthrough. The ratio of the pressure difference between the inlet and outlet

of the acid solution and the core pressure difference at the initial time is taken as the standard. When the ratio is 0.01, the acid solution breaks through the core. The definition of breakthrough volume (Panga et al., 2002) can be expressed as:

$$PV_{BT} = \frac{V_{acid}}{V_{ip}} = \frac{Q_{acid}T_{BT}}{V_{ip}} \quad (40)$$

where V_{acid} is consumption volume of injected acid solution, m³; V_{ip} is the initial pore volume of the core, m³; T_{BT} is the time taken for acid solution to break through the core, s; Q_{acid} is the acid solution injection rate, m³/s.

Unless otherwise specified, the values of all parameters are fixed. Under the wormhole dissolution pattern, we studied the effects of different shapes of vugs in the same area, different azimuth angles of vugs in the same area, different numbers of vugs in the same area, and different vugs distribution in the same area on the structure of dissolution wormhole and breakthrough volume of injected acid.

4.1 Effect of different shapes of vugs

In this section, we studied the influence of different shapes of vugs on acid-rock reactive flow. In the numerical simulation, the wormhole dissolution pattern with $Da = 250$ was selected. The shape of the vug is changed to observe its influence on the dissolution structure.

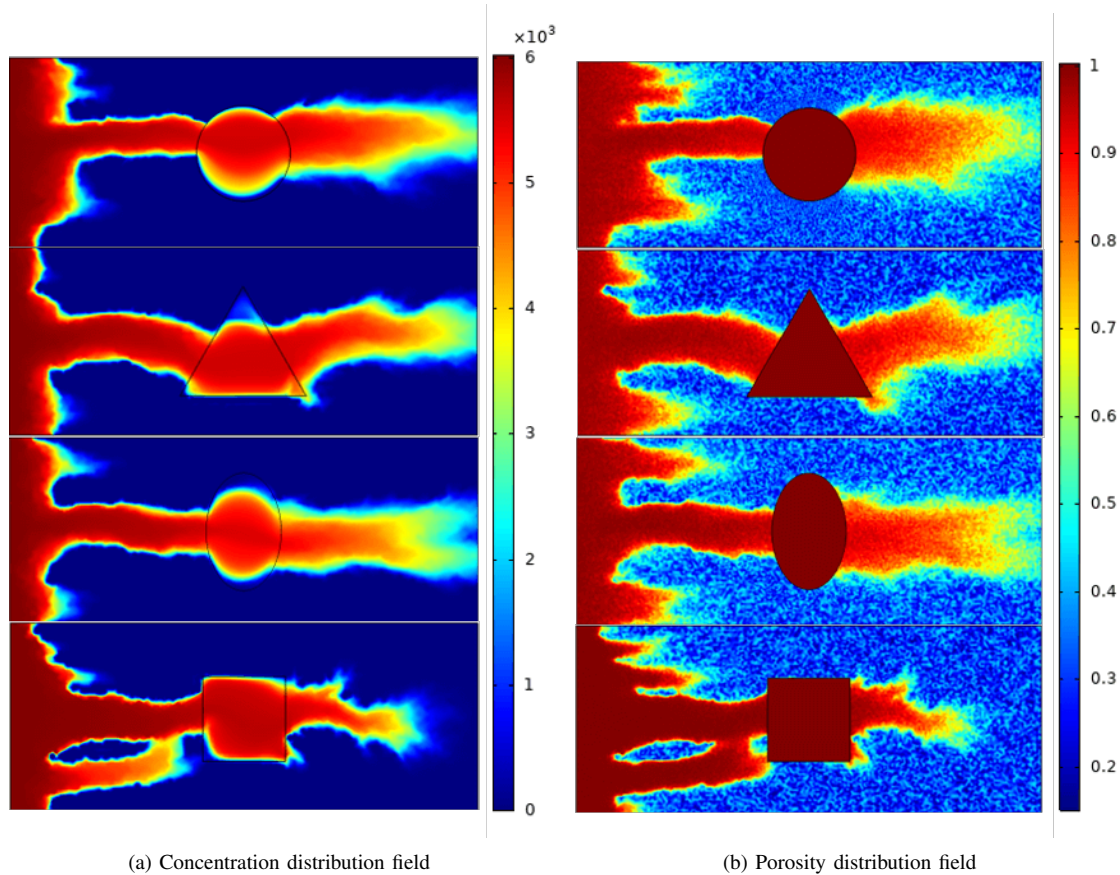


Fig. 1. Wormhole structure in the presence of different vug shapes.

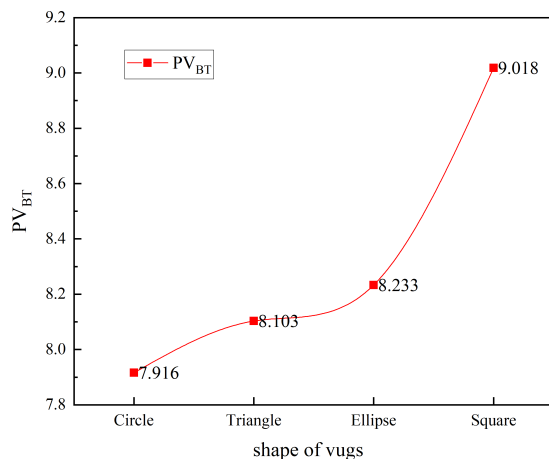


Fig. 2. Effect of the vug shapes on breakthrough volume.

The concentration distribution field and porosity distribution field is shown in Fig. 1. Fig. 1(b) illustrates that the shape of dissolution vugs has obvious influence on the distribution of wormhole at the entrance. Flow law of the fluid in the vugs belongs to free flow, and the diffusion of acid in the vugs is instantaneous. In this model, the gravity of fluid is not considered. The vug only provides flow, and the acid solution does not react in the vug. The acid solution flows along the direction with the maximum radius of the vug, contacts with

the matrix to form wormhole, and then continues to expand. It can be found that that the circular vug has the largest distance to reduce the effective path of acid solution in matrix and the shortest retention time of acid solution through comparing concentration distribution field and porosity distribution field of acid solution in matrix with the corresponding breakthrough volume diagram (Fig. 2).

4.2 Effect of azimuth of dissolution vugs

In this section, an elliptical vug is added to study the influence of azimuth angle of dissolution vug on the dissolution structure. The changes of porosity distribution field and concentration distribution field are observed by changing the azimuth angle of vugs.

Fig. 3 shows concentration distribution field and porosity distribution field. The results show that the azimuth angle of vug is closely related to the direction of wormhole. When the azimuth angle of the elliptical vug is 90° or 0° , the acid solution flows in from the left end and flows out from the right end. The azimuth angle of the vug has a strong control on the formation of subsequent wormholes, which results in the diameter of wormholes in the matrix is larger than that in other azimuth angles. When the azimuth angle of the elliptical vug is between 0° and 90° , the control effect of the vug on the formation of subsequent wormholes gradually weakens, which further reducing diameter of wormhole. Therefore, when the

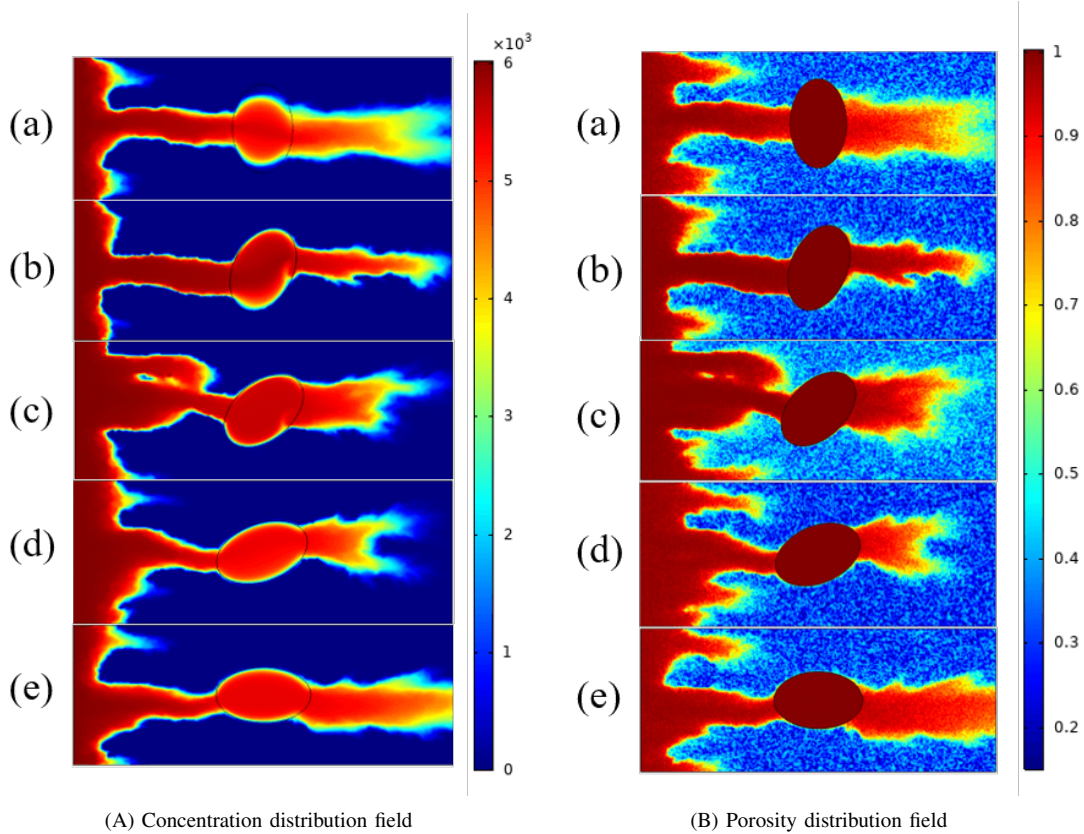


Fig. 3. Wormhole structure in the presence of different vug azimuth angles (a) 90°; (b) 67.5°; (c) 45°; (d) 22.5°; (e) 0°.

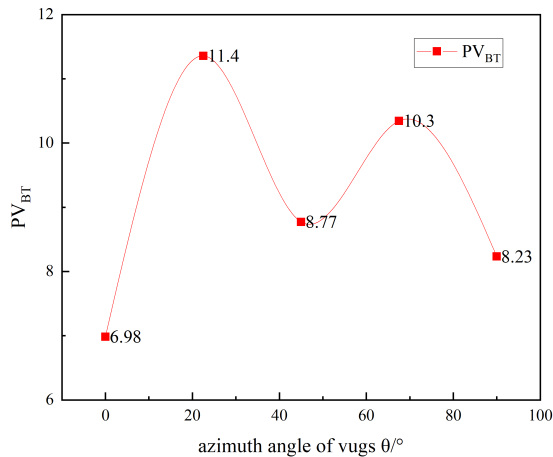


Fig. 4. Effect of the vug azimuth angles on breakthrough volume.

injection direction of acid solution is parallel or vertical to the azimuth angle of the vug, the dominant wormhole with stronger conductivity can be generated by acid injection.

Fig. 4 shows breakthrough volume diagram of acid solution with different vug azimuth angles. When the azimuth angle of the vug is vertical or parallel to the acid injection direction, the breakthrough volume of acid solution is small. When the azimuth angle of the vug is between 0° and 90°, the residence time of acid solution in the matrix increases strengthening acid consumption. When the azimuth angle of the vug is 0°, the

consumed acid solution is the minimum, and the corresponding acid breakthrough volume is the smallest.

4.3 Effect of different vug numbers

In this section, a varying numbers of vugs from 1 to 4 are set to study the effect of different vug numbers on the wormhole structure while keeping the total area of vug unchanged. The concentration distribution field and porosity distribution field obtained by the four models are shown in Fig. 5.

It can be observed from Fig. 5(B) that the number of vugs affects the distribution of wormhole at the initial injection end. With the increase of the number of vugs, the acid solution flows into the direction with the fastest pressure drop and the shortest effective flow path. The concentration distribution field diagram in Fig. 5(A) shows that when the acid solution penetrates the vug horizontally, it continues to penetrate the next vug and eventually forms a more complete wormhole.

Fig. 6 shows acid breakthrough volume diagram of the model with the same area and different number of vugs. The vug is an equipotential body. Although the total pore volume of the vug is the same, the flow distance and residence time of the acid solution in the horizontal direction are effectively shortened with the increase of the number of vugs in the horizontal direction. The injected acid consumed becomes less and less, and the breakthrough volume of the acid solution are also smaller. The largest breakthrough volume of acid solution

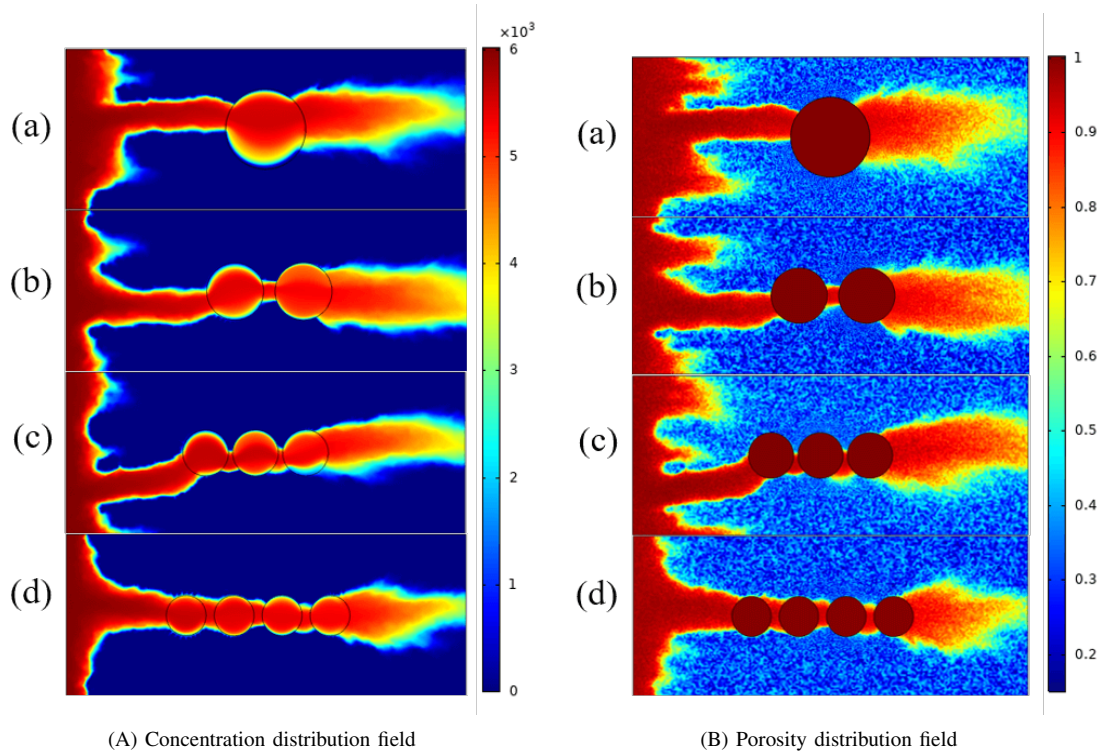


Fig. 5. Wormhole structure in the presence of the different number of vugs (a).model 1; (b). model 2; (c). model 3; (d). model 4.

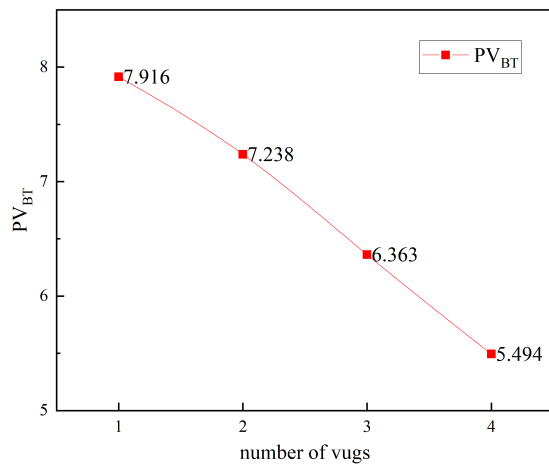


Fig. 6. Effect of the different number of vugs on breakthrough volume.

in model 1 is created by the minimum equivalent radius of vug and the minimum effective path of reducing acid solution in matrix. The breakthrough volume of acid solution in model 4 is the smallest and the amount of acid solution consumed is the least.

4.4 Effect of different spatial distribution

Five models are designed to study the effect of different spatial distribution of the same vug number and area on the wormhole structure. In the first three models, the vugs are arranged in a straight line in the horizontal direction, and there are three different positions distribution in the matrix.

In the latter two models, vugs are randomly distributed. The number and area of vugs in the five models were unchanged, only the location and distribution of vugs in the matrix were changed. The simulated concentration distribution field and porosity distribution field are shown in Fig. 7.

Fig. 7 shows that the distribution of vugs plays a huge role in guidance on the formation of wormholes and affects the distribution of wormhole structure in matrix. Because the flow of acid solution in the vug is free flow, the level of velocity is much larger than that in matrix. The diffusion velocity of acid solute in vugs is related to the convection diffusion velocity of acid solution, therefore, the diffusion of acid in vugs is instantaneous. When the acid solution first enters the vug, the concentration is lower than that in the matrix. As the acid solution continues to enter the vug, the concentration in the vug is gradually equal to that in the matrix. The vug becomes a part of wormhole and participates in the subsequent wormhole formation.

Fig. 8 shows the breakthrough volume diagram of each model acid solution in vug medium. When the vugs are distributed on the same horizontal line, the breakthrough volume of the injected acid solution is basically unchanged whether the vugs are distributed in the upper, middle or lower part of the matrix, and the breakthrough volume of the acid solution increases obviously when the vugs are randomly distributed.

5. Conclusion

In this work, a two-scale model is developed using dual domain method and discrete vugs model to carbonate acidizing process with existence of vugs. Darcy equation is employed

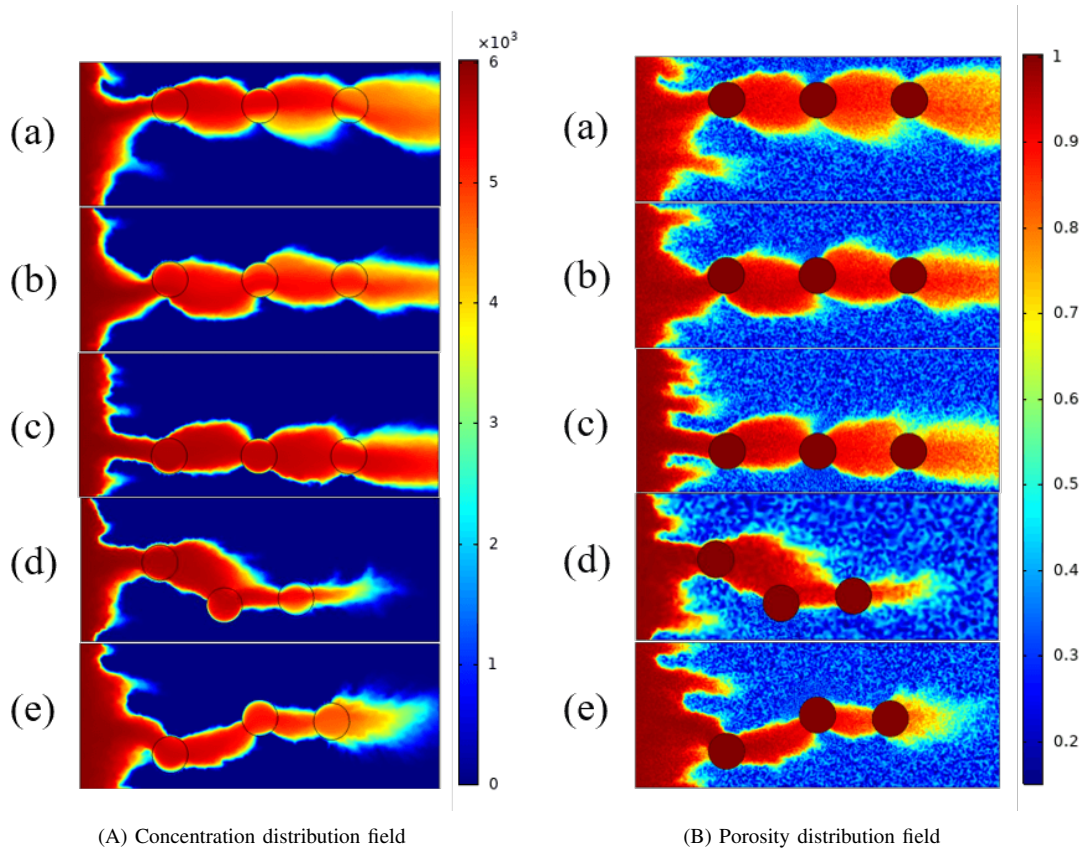


Fig. 7. Wormhole structure in the presence of the different vug distribution (a) model 1; (b) model 2; (c) model 3; (d) model 4; (e) model 5.

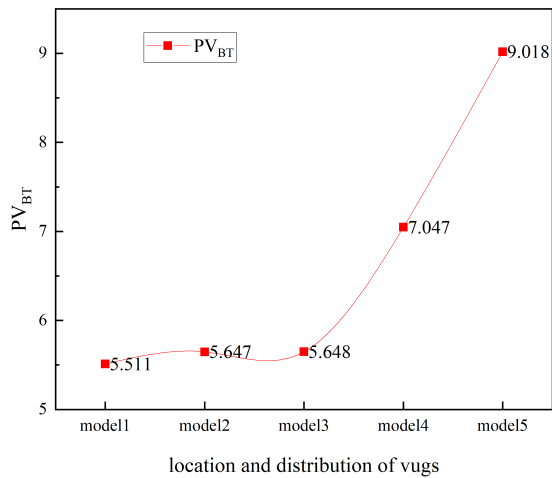


Fig. 8. Effect of the vug distribution on breakthrough volume.

in solid matrix region. Navier Stokes equation is adopted for free flow region in vugs. The modified Beavers-Joseph-Saffman (BJS) boundary condition is used to couple the two regions. The results show that the single vug can form a high velocity channel, which plays a role of high permeability strip. Besides, numerical cases are conducted to present the effect of vug characteristics, such as the shape, number, azimuth angle and spatial distribution of vugs, on acid-rock reaction process. The main conclusions include:

- 1) The shape of the vugs in the matrix not only affects the wormhole distribution at the initial injection end of the acid solution, but also affects the breakthrough volume of the injected acid. Circular vugs can effectively reduce the effective path of acid solution flow in the matrix, minimize the retention time, and breakthrough volume of acid solution in vug medium.
- 2) When the azimuth angle of the elliptical vug is 90° or 0°, the azimuth angle of the vug has a strong control on the formation of subsequent wormholes. When the azimuth angle of the elliptical vug is between 0° and 90°, the control effect of the vug on the formation of subsequent wormholes gradually weakens, which results in the diameter of wormhole becoming smaller.
- 3) Increasing vugs number in the horizontal direction shortens the effective flow distance of the acid solution in the horizontal direction and reduces the residence time of the acid solution in the vug medium and the breakthrough volume of the acid solution.
- 4) The breakthrough volume of the injected acid solution is independent to vugs distribution location when vugs are distributed on the same horizontal line. But, the random distribution of vugs increases the effective flow distance of acid solution in the matrix and the breakthrough volume of acid solution.

Acknowledgement

The authors would like to thank financial supported from Major Science and Technology Projects of China National Petroleum Corporation (ZD2019-183-008), National Natural Science Foundation of China (52074336), Fundamental Research Funds for the Central Universities (18CX05029A).

Conflict of interest

The authors declare no competing interest.

Open Access This article, published at Ausasia Science and Technology Press on behalf of the Division of Porous Flow, Hubei Province Society of Rock Mechanics and Engineering, is distributed under the terms and conditions of the Creative Commons Attribution (CC BY-NC-ND) license, which permits unrestricted use, distribution, and reproduction in any medium, provided the original work is properly cited.

References

- Ali, M.T., Ezzat, A.A., Nasr-El-Din, H.A. A model to simulate matrix-acid stimulation for wells in dolomite reservoirs with vugs and natural fractures. *SPE J.* 2020, 25(2): 609-631.
- Balakotaiah, V., West, D.H. Shape normalization and analysis of the mass transfer controlled regime in catalytic monoliths. *Chem. Eng. Sci.* 2002, 57(8): 1269-1286.
- Beavers, G.S., Joseph, D.D. Boundary conditions at a naturally permeable wall. *J. Fluid Mech.* 1967, 30(1): 197-207.
- Cai, J., Hu, X. *Petrophysical Characterization and Fluids Transport in Unconventional Reservoirs*. Amsterdam, Netherlands, Elsevier, 2019.
- Daccord, G., Lenormand, R., Liétard, O. Chemical dissolution of a porous medium by a reactive fluid-I. Model for the "wormholing" phenomenon. *Chem. Eng. Sci.* 1993, 48(1): 169-178.
- Fredd, C.N., Fogler, H.S. Influence of transport and reaction on wormhole formation in porous media. *AIChE J.* 1998, 44(9): 1933-1949.
- Fredd, C.N., Fogler, H.S. Optimum conditions for wormhole formation in carbonate porous media: Influence of transport and reaction. *SPE J.* 1999, 4(3): 196-205.
- Fredd, C.N., Miller, M.J. Validation of carbonate matrix stimulation models. Paper SPE 58713 Presented at SPE International Symposium on Formation Damage Control, Lafayette, Louisiana, 23-24 February, 2000.
- Fredd, C.N., Tjia, R., Fogler, H.S. The existence of an optimum damkohler number for matrix stimulation of carbonate formations. Paper SPE 38167 Presented at SPE European Formation Damage Conference, Hague, Netherlands, 2-3 June, 1997.
- Ghommem, M., Zhao, W., Dyer, S., et al. Carbonate acidizing: Modeling, analysis, and characterization of wormhole formation and propagation. *J. Pet. Sci. Eng.* 2015, 131: 18-33.
- Huang, Z. Theoretical study on multiscale modeling of two-phase flow based on discrete fracture-vug model. Qingdao, China University of Petroleum (East China), 2012. (in Chinese)
- Huang, Z., Gao, B., Yao, J. On the interface boundary conditions for the stokes-darcy coupling problem. *Scientia Sinica Physica, Mechanica & Astronomica* 2014, 44(2): 212-220. (in Chinese)
- Huang, Z., Yao, J., Li, Y., et al. Permeability analysis of fractured vuggy porous media based on homogenization theory. *Science China Technological Sciences* 2010, 53(3): 839-847. (in Chinese)
- Huang, Z., Yao, J., Li, Y., et al. Numerical calculation of equivalent permeability tensor for fractured vuggy porous media based on homogenization theory. *Commun. Comput. Phys.* 2011, 9(1): 180-204.
- Izgec, O., Zhu, D., Hill, A.D. Numerical and experimental investigation of acid wormholing during acidization of vuggy carbonate rocks. *J. Pet. Sci. Eng.* 2010, 74(1-2): 51-66.
- Kalia, N., Balakotaiah, V. Effect of medium heterogeneities on reactive dissolution of carbonates. *Chem. Eng. Sci.* 2009, 64(2): 376-390.
- Kang, Z., Yang, L., Ji, B., et al. Key technologies for eor in fractured-vuggy carbonate reservoirs. *Oil & Gas Geology* 2020, 41(2): 434-441. (in Chinese)
- Li, Y. *Development Theories and Methods of Fracture-vug Carbonate Reservoirs*. Pittsburgh, USA, Academic Press, 2017.
- Liu, P., Xue, H., Zhao, L., et al. Simulation of 3D multi-scale wormhole propagation in carbonates considering correlation spatial distribution of petrophysical properties. *J. Nat. Gas Sci. Eng.* 2016, 32: 81-94.
- Lund, K., Fogler, H.S., McCune, C.C. Acidization-I. The dissolution of dolomite in hydrochloric acid. *Chem. Eng. Sci.* 1973, 28(3): 691-700.
- Lund, K., Fogler, H.S., McCune, C.C., et al. Acidization-II. The dissolution of calcite in hydrochloric acid. *Chem. Eng. Sci.* 1975, 30(8): 825-835.
- Ma, Y., He, D., Cai, X., et al. Distribution and fundamental science questions for petroleum geology of marine carbonate in china. *Acta Petrologica Sinica* 2017, 33(4): 1007-1020. (in Chinese)
- MacQuarrie, K.T.B., Mayer, K.U. Reactive transport modeling in fractured rock: A state-of-the-science review. *Earth-Sci. Rev.* 2005, 72(3-4): 189-227.
- Maheshwari, P., Ratnakar, R., Kalia, N., et al. 3-D simulation and analysis of reactive dissolution and wormhole formation in carbonate rocks. *Chem. Eng. Sci.* 2013, 90: 258-274.
- McDuff, D., Shuchart, C.E., Jackson, S., et al. Understanding wormholes in carbonates: Unprecedented experimental scale and 3D visualization. *J. Pet. Technol.* 2010, 62(10): 78-81.
- Mosthaf, K., Baber, K., Flemisch, B., et al. A coupling concept for two-phase compositional porous-medium and single-phase compositional free flow. *Water Resour. Res.* 2011, 47(10): W10522.
- Nield, D.A., Bejan, A. *Convection in Porous Media*. Berlin, Germany, Springer, 2013.
- Panga, M.K.R., Balakotaiah, V., Ziauddin, M. Modeling, simulation and comparison of models for wormhole formation during matrix stimulation of carbonates.

- Paper SPE 77369 Presented at SPE Annual Technical Conference and Exhibition, San Antonio, Texas, 29 September-2 October, 2002.
- Panga, M.K.R., Ziauddin, M., Balakotaiah, V. Two-scale continuum model for simulation of wormholes in carbonate acidization. *AIChE J.* 2005, 51(12): 3231-3248.
- Qi, N., Chen, G., Liang, C., et al. Numerical simulation and analysis of the influence of fracture geometry on wormhole propagation in carbonate reservoirs. *Chem. Eng. Sci.* 2019, 198: 124-143.
- Saffman, P.G. On the boundary condition at the surface of a porous medium. *Stud. Appl. Math.* 1971, 50(2): 93-101.
- Taylor, G. A model for the boundary condition of a porous material. Part 1. *J. Fluid Mech.* 1971, 49(2): 319-326.
- Wang, S., Han, X., Dong, Y., et al. Mechanisms of reservoir pore/throat characteristics evolution during long-term waterflooding. *Adv. Geo-Energy Res.* 2017, 1(3): 148-157.
- Wang, Y., Hill, A.D., Schechter, R.S. The optimum injection rate for matrix acidizing of carbonate formations. Paper SPE 26578 Presented at SPE Annual Technical Conference and Exhibition, Houston, Texas, 3-6 October, 1993.
- Yang, L. The theory and method for development of carbonate fractured-cavity reservoirs in tahe oilfield. *Acta Petrologica Sinica* 2013, 34(1): 115-121. (in Chinese)
- Yao, J., Huang, Z., Wang, Z., et al. Mathematical model of fluid flow in fractured vuggy reservoirs based on discrete fracture-vug network. *Acta Petrologica Sinica* 2010, 31(5): 815-819+824. (in Chinese)
- Yuan, T., Wei, C., Zhang, C.S., et al. A numerical simulator for modeling the coupling processes of subsurface fluid flow and reactive transport processes in fractured carbonate rocks. *Water* 2019, 11(10): 1957.
- Zhang, T., Li, Z., Adenutsi, C.D., et al. A new model for calculating permeability of natural fractures in dual-porosity reservoir. *Adv. Geo-Energy Res.* 2017, 1(2): 86-92.
- Zhao, L., Wang, R., Liu, P., et al. Numerical simulation of wormhole propagation considering natural micro-fractures. *Reservoir Evaluation and Development* 2020, 10(2): 76-82. (in Chinese)
- Zheng, S., Yang, L., Zhang, H. Network model of fractured vuggy carbonate reservoir. *Journal of China University of Petroleum (Edition of Natural Science)* 2010, 34(3): 72-75+79. (in Chinese)